Mineralogical Magazine (2019), **83**, 261–267
doi:10.1180/mgm.2018.121

CAMBRIDGE UNIVERSITY PRESS

Article

Brandãoite, $[BeAl_2(PO_4)_2(OH)_2(H_2O)_4](H_2O)$, a new Be–Al phosphate mineral from the João Firmino mine, Pomarolli farm region, Divino das Laranjeiras County, Minas Gerais State, Brazil: description and crystal structure

Luiz A. D. Menezes Filho[1†], Mário L. S. C. Chaves[1], Mark A. Cooper[2], Neil A. Ball[2], Yassir A. Abdu[2,3], Ryan Sharpe[2], Maxwell C. Day[2] and Frank C. Hawthorne[2*]

[1]Federal University of Minas Gerais, Belo Horizonte, Minas Gerais, Brazil; [2]Department of Geological Sciences, University of Manitoba, Winnipeg, Manitoba R3T 2N2, Canada; and [3]Department of Applied Physics and Astronomy, University of Sharjah, P.O. Box 27272, Sharjah, United Arab Emirates

Abstract

Brandãoite, $[BeAl_2(PO_4)_2(OH)_2(H_2O)_4](H_2O)$, is a new Be–Al phosphate mineral from the João Firmino mine, Pomarolli farm region, Divino das Laranjeiras County, Minas Gerais State, Brazil, where it occurs in an albite pocket with other secondary phosphates, including beryllonite, atencioite and zanazziite, in a granitic pegmatite. It occurs as colourless acicular crystals <10 μm wide and <100 μm long that form compact radiating spherical aggregates up to 1.0–1.5 mm across. It is colourless and transparent in single crystals and white in aggregates, has a white streak and a vitreous lustre, is brittle and has conchoidal fracture. Mohs hardness is 6, and the calculated density is 2.353 g/cm^3. Brandãoite is biaxial (+), $\alpha = 1.544$, $\beta = 1.552$ and $\gamma = 1.568$, all ± 0.002; $2V_{obs} = 69.7(10)°$ and $2V_{calc} = 71.2°$. No pleochroism was observed. Brandãoite is triclinic, space group $P\bar{1}$, $a = 6.100(4)$, $b = 8.616(4)$, $c = 10.261(5)$ Å, $\alpha = 93.191(11)$, $\beta = 95.120(11)$, $\gamma = 96.863(11)°$, $V = 532.1(8)$ Å^3 and $Z = 2$. Chemical analysis of a 4 μm wide needle-shaped crystal by electron microprobe and secondary-ion mass spectrometry gave $P_2O_5 = 28.42$, $Al_2O_3 = 20.15$, $BeO = 4.85$, $H_2O = 21.47$ and sum = 74.89 wt.%. The empirical formula, normalised on the basis of 15 anions pfu with (OH) = 2 and (H_2O) = 5 apfu (from the crystal structure) is $Be_{0.98}Al_{1.99}P_{2.02}H_{12}O_{15}$. The crystal structure was solved by direct methods and refined to an R_1 index of 7.0%. There are two *P* sites occupied by P^{5+}, two *Al* sites occupied by octahedrally coordinated Al^{3+}, and one *Be* site occupied by tetrahedrally coordinated Be^{2+}. There are fifteen anions, two of which are (OH) groups and five of which are (H_2O) groups. The simplified ideal formula is thus $[BeAl_2(PO_4)_2(OH)_2(H_2O)_4](H_2O)$ with $Z = 2$. Beryllium and P tetrahedra share corners to form a four-membered ring. Aluminium octahedra share a common vertex to form an $[Al_2\varphi_{11}]$ dimer, and these dimers are cross-linked by P tetrahedra to form a complex slab of polyhedra parallel to (001). These slabs are cross-linked by $BeO_2(OH)(H_2O)$ tetrahedra, with interstitial (H_2O) groups in channels that extend along [100].

Keywords: brandãoite, new mineral, chemical analysis, beryllium phosphate, crystal structure, infrared spectrum, Minas Gerais State, Brazil

(Received 10 January 2018; accepted 6 March 2018)

Introduction

Brandãoite is a new Be–Al phosphate mineral from a granitic pegmatite in the Pomarolli farm region, Divino das Laranjeiras County, Minas Gerais State, Brazil. The mineral is named after Professor Paulo Roberto Gomes Brandão (born January 26, 1944), Department of Mining Engineering, Universidade Federal de Minas Gerais (UFMG). Dr. Brandão specialises in the mineralogical characterisation of ores and in the development of improved ore-concentration techniques, and freely allows access to his laboratory for the characterisation of unknown minerals. Both the mineral and the name have been approved by the Commission on New Minerals, Nomenclature and Classification of the International Mineralogical Association (IMA2016-071a, Menezes *et al.*, 2017). Holotype material is deposited in the collections of the Department of Natural History (Mineralogy), Royal Ontario Museum, 100 Queens Park, Toronto, Ontario M5S 2C6, Canada under catalogue number M57443.

Occurrence

Brandãoite was collected from a tabular- to lens-shaped pegmatite in the Pomarolli farm region, Divino das Laranjeiras County, Minas Gerais State, Brazil. This pegmatite body is known as the 'João Firmino mine', with coordinates 18°40′25"S, 41°29′27.5"W (or UTM 237250E, 7933450N, zone 24), and is located ca. 2 km to the northwest of the well-known Córrego Frio pegmatite,

*Author for correspondence: Frank Hawthorne, Email: frank_hawthorne@umanitoba.ca
†Deceased 2014

Associate Editor: Peter Leverett
Cite this article: Menezes Filho L.A.D., Chaves M.L.S.C., Cooper M.A., Ball N.A., Abdu Y.A., Sharpe R., Day M.C. and Hawthorne F.C. (2019) Brandãoite, $[BeAl_2(PO_4)_2(OH)_2(H_2O)_4](H_2O)$, a new Be–Al phosphate mineral from the João Firmino mine, Pomarolli farm region, Divino das Laranjeiras County, Minas Gerais State, Brazil: description and crystal structure. *Mineralogical Magazine* **83**, 261–267. https://doi.org/10.1180/mgm.2018.121

from which brazilianite, scorzalite and souzalite were first described. Together with dozens of other bodies, both pegmatites are included in the Galiléia-Mendes Pimentel pegmatite field (Chaves and Scholz, 2008). The João Firmino pegmatite is hosted in quartz-biotite schist belonging to the São Tomé Formation, Rio Doce Group, of Neoproterozic age. Pegmatogenesis in this region is attributed to residual material from S-type granitic intrusions associated with the Araçuaí orogeny between 630 and 490 Ma (Pedrosa-Soares *et al.*, 2011). The João Firmino pegmatite is a highly fractionated member of a series of LCT pegmatites that intruded into tectonised micaschist country rock.

Associated minerals

Besides quartz, microcline, albite, beryl, green tourmaline, spodumene and muscovite, the following phosphate-assemblage minerals have been described from the João Firmino pegmatite: montebrasite, autunite, brazilianite, childrenite–eosphorite, fluorapatite, phosphosiderite, frondelite, gormanite, heterosite–purpurite, hydroxylherderite, moraesite and roscherite–zanazziite (Chaves *et al.*, 2005, 2008). Brandãoite was discovered in an albite pocket with other secondary phosphates, including beryllonite, atencioite and zanazziite.

Origin

Secondary pegmatite phosphates from the Divino das Laranjeiras-Mendes Pimentel field are the result of secondary alteration of primary triphylite and/or montebrasite. The João Firmino pegmatite, as well as other important mines on the Pomarolli farm (Córrego Frio, Telírio, Jove Lauriano, Pomarolli, etc.), are products of montebrasite alteration (Scholz *et al.*, 2012).

Physical properties

Brandãoite occurs as colourless acicular crystals <10 μm wide and <100 μm long that form compact radiating spherical aggregates up to 1.0–1.5 mm across. Individual fibres within the aggregates generally consist of complex interpenetrating crystals in parallel growth about the fibre axis (Fig. 1*a*). Rare single crystals are elongated along [100] and are terminated by (0*kl*) faces that are too small to index but are possibly {001}, {011} and {01$\bar{1}$} pinacoids, forming psuedo-hexagonal prisms (see the upper crystal in Fig. 1*b*, and Fig. 1*c*). The flattening orientation is perpendicular to {001} (Fig. 1*a*, lower crystal in Fig. 1*b*). Brandãoite is colourless and transparent in single crystals and white in aggregates, and has a white streak and a vitreous lustre. It does not fluoresce in ultraviolet light. Cleavage and parting were not observed, it is brittle and has a conchoidal fracture. Mohs hardness is 6, and the calculated density is 2.353 g/cm^3 (from the empirical formula). To measure the optical properties, a crystal was mounted on a Bloss spindle stage and the extinction curves were measured using white light. The resulting measurements were processed using *Excalibr II* (Bartelmehs *et al.*, 1992) and the 2V angle was derived. Brandãoite is biaxial (+). *Excalibr II* also provided the setting angles for measurement of refractive indices: α = 1.544, β = 1.552, γ = 1.568, all ± 0.002; $2V_{obs}$ = 69.7(10)°, $2V_{calc}$ = 71.2°. No pleochroism was observed. The optic orientation was measured by transferring the crystal and goniometer head from the spindle stage to a single-crystal diffractometer and orienting the crystallographic axes (Gunter and Twamley, 2001); the orientation is given in Table 1. The Gladstone-Dale compatibility index is –0.019 (excellent, Mandarino, 1981), using d_{calc} and the ideal chemical composition.

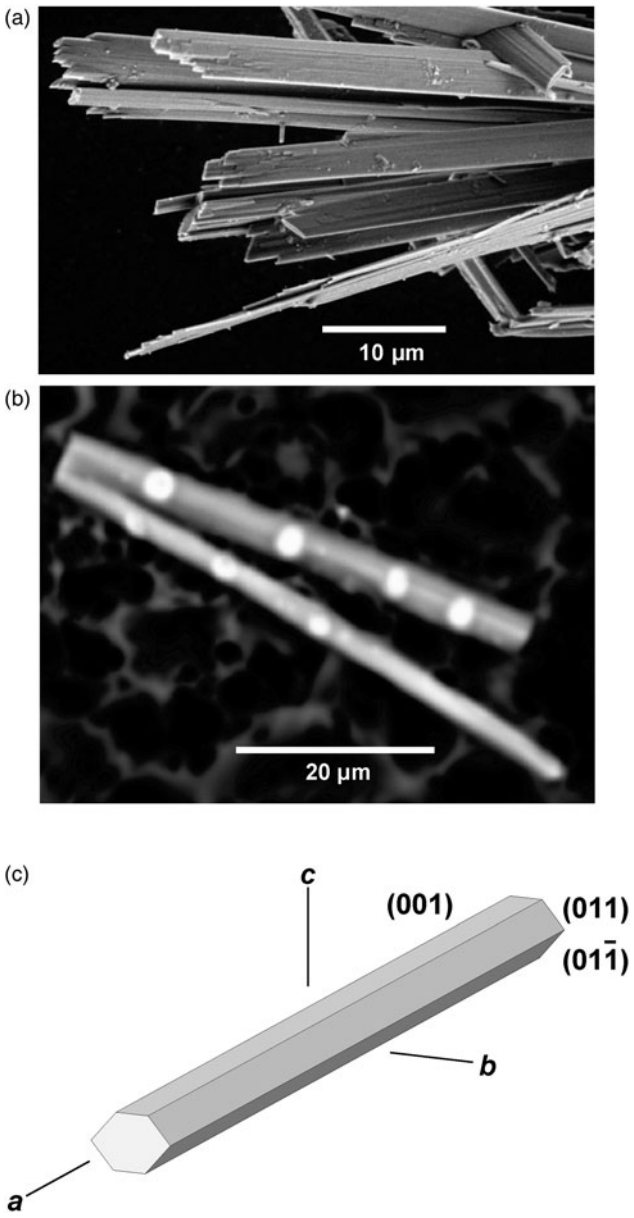

Fig. 1. Scanning electron microscopy images of brandãoite: (*a*) lath-like flattened prisms and (*b*) image of two crystals in the section used for electron microprobe analysis; and (*c*) morphology of an ideal crystal.

Table 1. Optical orientation (°) of brandãoite.

	a	*b*	*c*
X	87.6	124.0	31.2
Y	54.0	136.4	118.8
Z	143.9	113.8	101.1

Chemical composition

Two crystals of brandãoite (~50 μm long and 4 μm wide, Fig. 1*b*) were laid down on the surface of a plexiglass disk, anchored with a

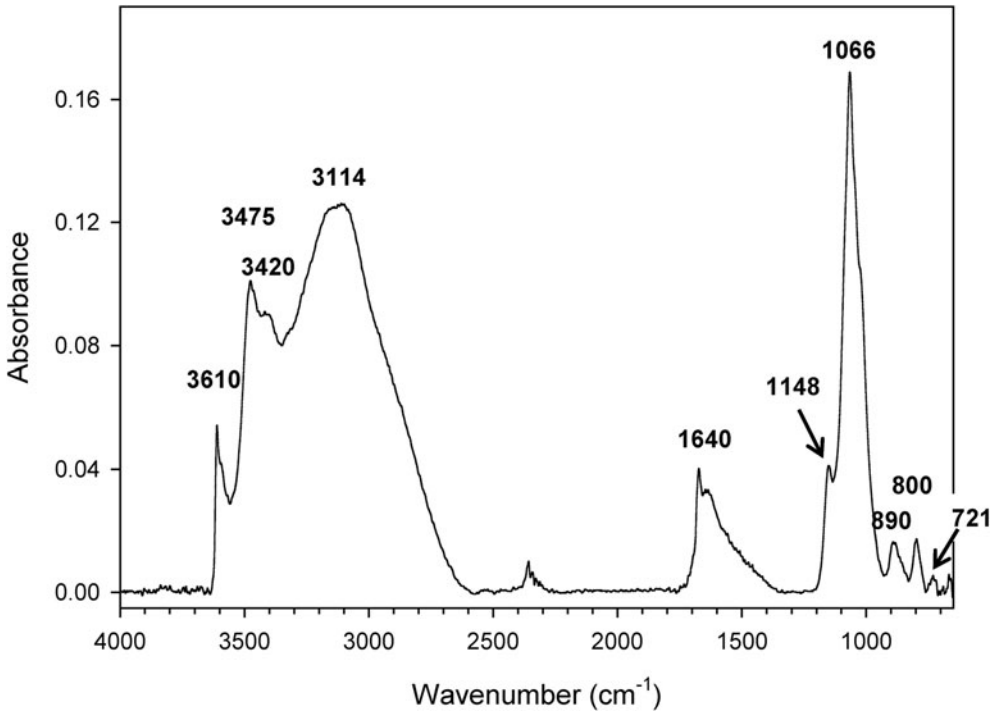

Fig. 2. Infrared spectrum of brandãoite.

minute application of epoxy, and carbon coated. A focused electron-beam was used due to the narrow crystal width, and a low beam-current was used (5 nA) due to the beam-sensitive nature of the mineral. The crystals were analysed with a Cameca SX100 electron microprobe operated in wavelength-dispersive mode at 15 kV and 5 nA, and using a beam diameter of 1 μm. Brazilianite was used as the standard for P and Al. Three analyses were acquired along the crystal, and following each analysis, significant beam damage could be seen at each acquisition point (Fig. 1*b*). The upper surface of the crystal contains sloping sides, and the circumference of beam-damage demarcation extends onto the sloping sides. The low analytical total can be attributed to a combination of variable surface attitude and activation volumes that exceed the bounds of the crystal (note: the three analyses from the narrower adjacent crystal give analytical totals that are further reduced by ~10%, and are not included here). Despite the low analytical total (Table 2), the resultant Al:P stoichiometery is very close to its ideal 1:1 ratio from structure refinement. An energy-dispersive spectroscopy spectra showed that only P and Al are present. For the simplified formula $[BeAl_2(PO_4)_2(OH)_2(H_2O)_4](H_2O)$, the ideal wt.% oxides are BeO 6.63, Al_2O_3 27.04, P_2O_5 37.65, H_2O 28.67, total 100.00. Hawthorne and Grice (1990) proposed that crystal-structure solution and refinement, as an electron-counting technique, is a valid method of chemical analysis. The *Be* site in brandãoite gives a refined site-scattering value of 4.08(12) electrons and is tetrahedrally coordinated by O atoms from 1.600–1.679 Å with a <*Be*–O> distance of 1.632 Å, close to the grand <Be–O> distance of 1.633 Å given by Hawthorne and Huminicki (2002) for minerals and 1.637 Å given for 161 BeO_4 tetrahedra in minerals and inorganic structures by Gagné and Hawthorne (2016). The well-ordered remaining part of the structure requires that the *Be* site carry a 2+ charge for electroneutrality; this condition (encompassing the refined site-scattering value, the observed mean bond length and the requirement of electroneutrality) can be met only *via* occupancy of the *Be* site by Be. Subsequent to the derivation of the Be content as described above, secondary-ion mass spectrometry (CAMECA 7f SIMS) was used to analyse Be using a 2 nA primary beam of O^- ions accelerated at 12.5 kV. The diameter of the crystals is ~4 μm on average, much too small for conventional analysis by SIMS. Here, we analysed small clusters of crystals and derived the Be content using P as an internal standard. The primary beam was focused to ~30 μm, and a mass-resolving power of 700 and a –50 V sample offset were used to minimise interferences. The Be value acquired is in accord with the 1 apfu Be content derived from structure refinement. Brandãoite, ideally $[BeAl_2(PO_4)_2(OH)_2(H_2O)_4](H_2O)$, is one of the first Be–Al phosphate minerals to be described, the other being lefontite, ideally $Fe_2Al_2Be(PO_4)_2(OH)_6$ (Yang *et al.*, 2015).

Table 2. Chemical composition (wt.%) for brandãoite.

Constituent	Wt.%	Range
Al_2O_3	20.15(54)	19.39–20.64
P_2O_5	28.42(65)	27.63–29.21
BeO	4.85(16)	4.72–5.08
H_2O^*	21.47	–
Total	74.89	

Infrared spectroscopy

The Fourier-transform infrared (FTIR) spectrum was collected using a Bruker Hyperion 2000 IR microscope equipped with a liquid-nitrogen-cooled mercury-cadmium-telluride detector. The

Table 3. Simulated powder X-ray diffraction data (from single-crystal data) for brandãoite.

$I_{(meas.)}$ %	$d_{(meas.)}$ Å	*h k l*	$I_{(meas.)}$ %	$d_{(meas.)}$ Å	*h k l*
23	10.197	0 0 1	21	2.154	2 0 $\bar{3}$
82	**6.772**	**0 $\bar{1}$ 1**		2.153	2 $\bar{3}$ 1
30	6.339	0 1 1	21	2.134	0 4 0
6	6.028	1 0 0	25	2.117	0 $\bar{4}$ 1
85	**5.243**	**$\bar{1}$ 1 0**	13	2.100	1 $\bar{2}$ 4
34	5.099	0 0 2		2.096	$\bar{1}$ 4 0
73	**4.982**	**1 0 1**	11	2.046	$\bar{2}$ 0 4
12	4.746	$\bar{1}$ 1 1		2.043	$\bar{2}$ 3 2
20	4.657	1 1 0	10	2.034	2 $\bar{2}$ 3
41	4.512	0 $\bar{1}$ 2	8	2.014	0 $\bar{1}$ 5
12	4.426	$\bar{1}$ $\bar{1}$ 1	9	1.955	$\bar{2}$ $\bar{3}$ 1
100	**4.268**	**0 2 0**	18	1.936	3 0 1
48	**3.846**	**0 2 1**		1.936	$\bar{1}$ $\bar{4}$ 1
40	3.719	1 0 2		1.934	$\bar{3}$ 0 2
20	3.646	$\bar{1}$ $\bar{1}$ 2	15	1.926	$\bar{3}$ 1 2
15	3.579	1 $\bar{1}$ 2	8	1.912	$\bar{3}$ 2 0
30	3.484	1 $\bar{2}$ 1	9	1.905	1 3 3
34	3.399	0 0 3		1.903	3 1 0
17	3.262	1 1 2	8	1.892	$\bar{2}$ $\bar{3}$ 2
53	**3.091**	**$\bar{1}$ 0 3**		1.890	0 $\bar{2}$ 5
	3.087	0 1 3	19	1.867	2 $\bar{1}$ 4
14	3.043	1 2 1		1.864	0 $\bar{4}$ 3
13	3.014	2 0 0		1.862	$\bar{1}$ $\bar{3}$ 4
12	2.997	1 $\bar{2}$ 2		1.860	2 0 4
38	2.961	$\bar{2}$ 1 0	8	1.825	$\bar{2}$ 4 1
42	2.909	$\bar{1}$ $\bar{2}$ 2	6	1.810	1 $\bar{4}$ 3
68	**2.789**	**0 $\bar{3}$ 1**	8	1.796	1 1 5
76	**2.712**	**$\bar{2}$ 0 2**	9	1.771	2 1 4
	2.707	$\bar{1}$ 3 0		1.770	$\bar{2}$ 0 5
38	2.644	1 2 2	11	1.755	0 4 3
29	2.630	1 $\bar{3}$ 1	8	1.742	$\bar{3}$ $\bar{1}$ 3
31	2.603	$\bar{1}$ 3 1		1.739	$\bar{2}$ 1 5
11	2.576	0 2 3	26	1.699	$\bar{1}$ 5 0
	2.573	2 1 1	9	1.687	1 $\bar{5}$ 1
13	2.558	0 $\bar{3}$ 2		1.686	$\bar{2}$ 3 4
	2.549	0 0 4	11	1.675	$\bar{3}$ 3 2
14	2.513	2 $\bar{2}$ 1	7	1.665	$\bar{1}$ 5 1
19	2.491	2 0 2	6	1.637	$\bar{1}$ 1 6
	2.489	0 $\bar{1}$ 4		1.637	$\bar{2}$ $\bar{3}$ 4
11	2.457	1 3 0	8	1.627	$\bar{2}$ $\bar{2}$ 5
16	2.399	0 1 4	10	1.618	2 0 5
19	2.373	$\bar{2}$ 2 2	8	1.596	1 0 6
	2.371	$\bar{1}$ 3 2	8	1.591	1 5 0
12	2.327	$\bar{2}$ $\bar{2}$ 1		1.590	3 1 3
11	2.308	2 1 2	4	1.582	$\bar{3}$ 3 3
13	2.255	$\bar{2}$ $\bar{1}$ 3	21	1.552	$\bar{3}$ 4 1
5	2.217	2 2 1		1.551	1 5 1
			13	1.544	1 $\bar{5}$ 3

The strongest lines are given in bold.

spectrum in the range 4000–650 cm^{-1} was obtained by averaging 100 scans with a resolution of 4 cm^{-1}. The infrared spectrum of brandãoite is shown in Fig. 2. In the 4000–2600 cm^{-1} region (Fig. 2), there are two sharp bands at 3610 and 3475 cm^{-1} (with a shoulder at ~3420 cm^{-1}) attributable to stretching vibrations of OH groups, and a broad band centred at ~3114 cm^{-1} which is due to H_2O stretches. The H_2O bending mode is observed at ~1640 cm^{-1}. In the low-frequency region, bands at 1066 cm^{-1} (very strong) with a shoulder at 1148 cm^{-1} are assigned to stretching vibrations of the PO_4 group, and the peaks at ~890, 800 and 721 cm^{-1} may be assigned to *M*–OH stretches.

Powder X-ray diffraction

Brandãoite is available in an almost vanishingly small amount. Thus we collapsed the single-crystal X-ray intensity data to

Table 4. Miscellaneous Information for brandãoite.

Crystal data	
Crystal size (μm)	3 × 4 × 80
Crystal system, space group	$P\bar{1}$
Temperature (K)	293
a, *b*, *c* (Å)	6.100(4), 8.616(4), 10.261(5)
α, β, γ (°)	93.191(11), 95.120(11), 96.863(11)
V (Å^3)	532.1(8)
Z	2
Density(from the empirical formula) (g/cm)^3	2.353
Data collection	
Crystal description	Colourless prism
Instrument	Bruker D8 rotating-anode 3-circle
Radiation type, wavelength (Å)	Mo*K*α
Number of frames	8800
θ range (°)	2–25
Absorption correction	Empirical (*SADABS*, Sheldrick 2008)
T_{min}, T_{max}	0.7838, 0.9801
No. of reflections	13,240
No. in Ewald sphere	3764
R_{int} (%)	4.61
No. unique reflections	1887
No. with ($F_o > 4\sigma F$)	1319
Indices range of *h*, *k*, *l*	$-7 \le h \le 7$, $-10 \le k \le 10$, $-12 \le l \le 12$
Refinement	
Refinement	least-squares
R_1 (%)	6.97
wR_2 (%)	19.78
GoF	1.086
No. of refined parameters	202
$\Delta\rho_{max}$, $\Delta\rho_{min}$ (e^- Å^{-3})	1.30, −1.04
Cell content:	2 $[BeAl_2(PO_4)_2(OH)_2(H_2O)_5]$

$R_1 = \Sigma(|F_o| - |F_c|) / \Sigma|F_o|$
$wR_2 = [\Sigma w (F_o^2 - F_c^2)^2 / \Sigma w (F_o^2)^2]^{1/2}$, $w = 1 / [\sigma^2(F_o^2) + (0.13P)^2 + 0.00P]$ where $P = (\mathrm{Max}(F_o^2,0) + 2F_c^2) / 3$

Table 5. Atom positions and displacement parameters (Å)^2 for brandãoite.

Site	*x*	*y*	*z*	U_{eq}
Be	0.8113(14)	0.1403(11)	0.5481(8)	0.0128(16)
*P*1	0.3941(3)	0.67098(19)	0.11998(16)	0.0084(5)
*P*2	0.0332(3)	0.1053(2)	0.31480(16)	0.0100(5)
*Al*1	0.3609(3)	0.2927(2)	0.14081(18)	0.0099(5)
*Al*2	0.9153(3)	0.7678(2)	0.17968(19)	0.0092(5)
O1	0.2206(7)	0.7804(5)	0.1484(4)	0.0118(10)
O2	0.3132(7)	0.5055(5)	0.1575(4)	0.0121(9)
O3	0.6105(7)	0.7374(5)	0.2021(4)	0.0125(10)
O4	0.4214(7)	0.6633(5)	−0.0278(4)	0.0126(10)
O5	0.1473(8)	0.2517(6)	0.2590(4)	0.0141(9)
O6	0.2017(8)	0.0378(6)	0.4082(4)	0.0136(10)
O7	−0.0672(7)	−0.0127(5)	0.2007(4)	0.0128(10)
O8	−0.1552(7)	0.1535(5)	0.3930(4)	0.0135(10)
OH1	0.9979(7)	0.7540(5)	0.3581(4)	0.0130(10)
OH2	0.1491(8)	0.2256(5)	0.0036(4)	0.0140(10)
OW1	0.5578(8)	0.1953(6)	0.5568(5)	0.0155(10)
OW2	0.5844(8)	0.3414(6)	0.2868(5)	0.0158(10)
OW3	0.4498(8)	0.0780(6)	0.1478(5)	0.0185(10)
OW4	0.8955(8)	0.5386(6)	0.1648(5)	0.0156(10)
OW5	0.2340(11)	0.4617(8)	0.4874(6)	0.0427(14)
H1	0.516(15)	0.204(11)	0.647(3)	0.05*
H2	0.424(8)	0.150(10)	0.502(7)	0.05*
H3	0.684(12)	0.285(9)	0.341(7)	0.05*
H5	0.350(13)	−0.019(6)	0.154(10)	0.05*
H6	0.607(4)	0.063(12)	0.158(9)	0.05*
H7	0.034(8)	0.492(10)	0.181(9)	0.05*
H8	0.810(13)	0.463(9)	0.099(7)	0.05*

Note: H4 and H9–H12 were not located in the difference-Fourier map; * fixed during refinement.

Table 6. Selected interatomic distances (Å) and angles (°) for brandãoite.

Be–O6	1.618(10)	*P*1–O1	1.535(5)	*P*2–O5	1.532(5)
Be–O8	1.631(10)	*P*1–O2	1.533(5)	*P*2–O6	1.530(5)
Be–OH1	1.600(10)	*P*1–O3	1.532(5)	*P*2–O7	1.539(5)
Be–OW1	1.679(10)	*P*1–O4	1.539(5)	*P*2–O8	1.542(5)
<*Be*–Φ>	1.632	<*P*1–O>	1.535	<*P*2–O>	1.536
*Al*1–O2	1.892(5)	*Al*2–O1	1.909(5)		
*Al*1–O4	1.859(5)	*Al*2–O3	1.883(5)		
*Al*1–O5	1.874(5)	*Al*2–O7	1.881(5)		
*Al*1–OH2	1.841(5)	*Al*2–OH1	1.869(5)		
*Al*1–OW2	1.925(5)	*Al*2–OH2	1.892(5)		
*Al*1–OW3	1.992(6)	*Al*2–OW4	1.961(5)		
<*Al*1–Φ>	1.897	<*Al*2–Φ>	1.899		

Table 7. Proposed H bonding (Å and °) in brandãoite.

OH1–OW5	2.841(8)				
OH2–O7	3.215(7)				
OW1–O3	2.819(6)	H1···O3	1.87(3)	OW1–H1–O3	164(8)
OW1–O6	2.713(7)	H2···O6	1.742(18)	OW1–H2–O6	170(8)
O3–OW1–O6	103.4(2)				
OW2–O8	2.615(7)	H3···O8	1.66(3)	OW2–H3–O8	163(9)
OW2–OW4	2.819(7)				
O8–OW2–OW4	100.0(2)				
OW3–O1	2.771(7)	H5···O1	1.81(2)	OW3–H5–O1	166(9)
OW3–O7	3.146(7)	H6···O7	2.18(2)	OW3–H6–O7	169(8)
O1–OW3–O7	97.9(2)				
OW4–O2	2.605(7)	H7···O2	1.74(5)	OW4–H7–O2	146(8)
OW4–O4	2.679(7)	H8···O4	1.75(4)	OW4–H8–O4	156(8)
O2–OW4–O4	120.9(2)				
OW5–OW5	3.217(13)				
OW5–O5	2.850(8)				
OW5–OW5–O5	102.4(3)				

produce an experimental diffraction pattern that simulates that of a powder pattern (in much the same way as a Gandolfi camera). The pattern is reported in Table 3.

Crystal structure: data collection, structure solution and refinement

A single crystal (3 μm x 4 μm x 80 μm) was attached to a tapered glass fibre and mounted on a Bruker D8 three-circle diffractometer equipped with a rotating anode generator (Mo*K*α X-radiation), multilayer optics and an APEX-II detector. In excess of a Ewald sphere of data was collected to 50°2θ using 60 s per 0.2° frame with a crystal-to-detector distance of 5 cm. The combination of low mean-scattering-power and small crystal volume resulted in a low-intensity diffraction pattern, with only very weak reflections occupying the outer 40–50°2θ shell. A total of 13,240 reflections was integrated, empirical absorption corrections (*SADABS*, Sheldrick 2008) were applied and identical reflections were averaged, resulting in 3764 individual reflections within the Ewald sphere. The final unit-cell (Table 4) is based on least-squares refinement of 2115 reflections ($I > 7\sigma I$). The intensity data were merged in the space group $P\bar{1}$ to give 1887 unique reflections ($R_{merge} = 4.6\%$), and the crystal structure was solved using direct methods. The refinement model contains one *Be* site, two *P* sites, two *Al* sites and fifteen anion sites, and the refined site-scattering values (Hawthorne *et al.*, 1995) and mean bond lengths collectively support complete chemical order over all cation sites. Two (OH) groups and five (H_2O) groups were identified using bond-valence arguments, and seven of the possible twelve H positions were located in reasonable positions in the difference-Fourier map, and inserted into the structure-refinement model. Of the 1887 unique reflections, 1319 were classed as observed [$F_o > 4\sigma F$], and the structure refined to an *R* value of 7.0% for a fully anisotropic model for all non-H atoms. The displacement parameter at the OW5 site is approximately three times the magnitudes of the displacement parameters at the OW1–4 sites. Either (1) the occupancy of the OW5 site is <1.00, or (2) the (H_2O) group at the OW5 site has much larger displacements than the other (H_2O) groups as it is only held in the structure by hydrogen bonds to other anions in the structure. For simplicity, we have adopted possibility (1) while recognising that possibility (2) is equally likely given the result of the refinement. Atom positions and equivalent-isotropic-displacement parameters are given in Table 5, selected interatomic distances are given in Table 6, proposed H-bonding is given in Table 7, and bond-valences are given in Table 8. A crystallographic

Table 8. Bond-valence (vu)* table for brandãoite.

Site	*Be*	*P*1	*P*2	*Al*1	*Al*2	Σ	H1	H2	H3	H4	H5	H6	H7	H8	H9	H10	H11	H12	Σ
O1		1.25			0.49	1.74					0.2								1.94
O2		1.26		0.52		1.78							0.2						1.98
O3		1.26			0.53	1.79	0.2												1.99
O4		1.24		0.56		1.80								0.2					2.00
O5			1.26	0.54		1.80									0.2				2.00
O6	0.53		1.27			1.80		0.2											2.00
O7			1.24		0.53	1.77						0.1						0.1	1.97
O8	0.51		1.23			1.74			0.2										1.94
OH1	0.56				0.55	1.11											0.8		1.91
OH2				0.59	0.52	1.11												0.9	2.01
OW1	0.43					0.43	0.8	0.8											2.03
OW2				0.47		0.47			0.8	0.8									2.07
OW3				0.40		0.40					0.8	0.9							2.10
OW4					0.43	0.43				0.2			0.8	0.8					2.23
OW5						0									0.8	0.9	0.2		2.00
																0.1			
Σ	2.03	5.01	5.00	3.08	3.05		1.0	1.0	1.0	1.0	1.0	1.0	1.0	1.0	1.0	1.0	1.0	1.0	

*Calculated using the parameters of Gagné and Hawthorne (2015).

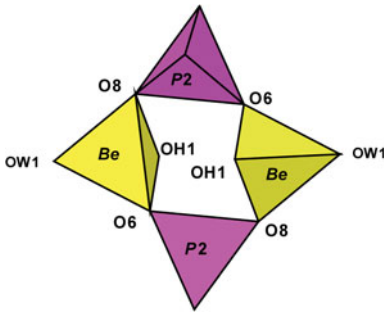

Fig. 3. The four-membered ring of alternating [BeO_2{OH}{H_2O}] and (PO_4) tetrahedra in brandãoite. Key: purple = (PO_4) tetrahedra and yellow = [BeO_2{OH}{H_2O}] tetrahedra.

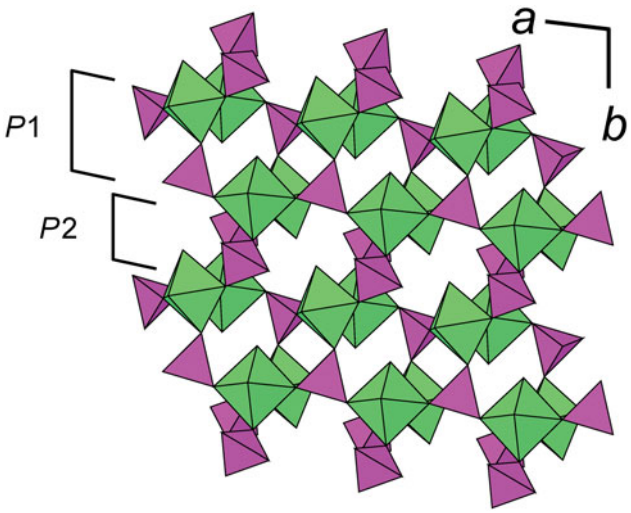

Fig. 4. The slab of [$Al_2\varphi_{11}$] dimers and (PO_4) tetrahedra projected onto (*h*0*l*); purple = (PO_4) tetrahedra; green = [Al_2O_{10}(OH)] dimers.

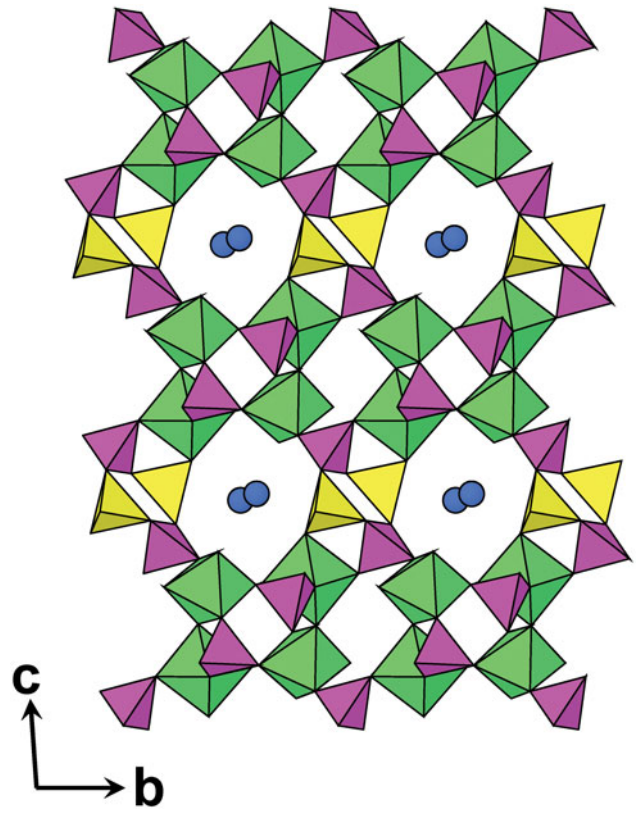

Fig. 5. The structure of brandãoite projected down [100], showing the slabs of Fig. 4 linked in the **c** direction by (BeO_2{OH}{H_2O}) tetrahedra, with OW5 (H_2O) groups (blue circles) in the interstices.

information file has been deposited with the Principal Editor of *Mineralogical Magazine* and is available as Supplementary material (see below).

Crystal structure: Description

In the crystal structure of brandãoite, there is a single *Be* site tetrahedrally coordinated by four anions with a <*Be*–Φ> distance (Φ unspecified anion) of 1.632 Å (Table 4) and a refined site-scattering equivalent to 4 electrons per site, consistent with full occupancy by Be^{2+}. There are two *P* sites tetrahedrally coordinated by four anions with <*P*–O> distances of 1.535 and 1.536 Å, close to the value of 1.537 Å given by Huminicki and Hawthorne (2002) for minerals, and close to the value of 1.537 Å given by Gagné and Hawthorne (2017*a*) for ordered minerals and inorganic compounds. The refined site-scattering values are equivalent to 15 electrons per site, consistent with full occupancy by P^{5+}. There are two *Al* sites octahedrally coordinated by six anions with <*Al*–Φ> distances of 1.897 and 1.899 Å, close to the value of 1.903 Å given by Gagné and Hawthorne (2017*b*) for ordered minerals and inorganic compounds. The refined site-scattering values are equivalent to 13 electrons per site, consistent with full occupancy by Al^{3+}. The anions O1–O8 each bond to one P atom and either one Be or one Al atom, and are therefore O^{2-} anions that additionally receive one or two weak hydrogen bonds (Tables 7, 8). The OH1 anion bonds to one Al atom and one Be atom, and the OH2 anion bonds to two Al atoms; these anions receive ~1.1 vu (valence units) from the bonded cations, and additionally have a H atom attached to form an (OH) group. The OW1–OW4 anions are bonded to either Be or Al atoms, and additionally have two attached H atoms, forming (H_2O) groups. The OW5 anion is not bonded to any cations, and is an interstitial (H_2O) group located within a structural channel.

The Be and P tetrahedra share corners to form a four-membered ring (Fig. 3) that is a common feature in many Be phosphate minerals. The Al1 and Al2 octahedra share a common OH2 vertex to form an [$Al_2\varphi_{11}$] dimer (φ = unspecified anion), and these dimers are cross-linked by P tetrahedra to form a complex slab of polyhedra, oriented parallel to (001) (Fig. 4). The P1 tetrahedra share all four of their vertices with neighbouring Al octahedra, whereas the P2 tetrahedra share two vertices with neighbouring Al octahedra and the other two vertices project outward from the upper and lower surfaces of the slab. Three (H_2O) groups [OW2, OW3 and OW4], attached to the Al dimers, project into void regions of the slab, and are involved in additional hydrogen bonding (not shown). The two vertices of the P2 tetrahedron that project outward from the slab [O6 and O8] are cross-linked by $BeO_2(OH)(H_2O)$ tetrahedra (Figs 4, 5), and the interstitial (H_2O) groups located at OW5 occur in channels that extend along [100] (Fig. 5).

Supplementary material. To view supplementary material for this article, please visit https://doi.org/10.1180/mgm.2018.121

Acknowledgements. We thank Ian Grey and Pete Leverett for their helpful comments on this paper. This work was supported by a Discovery grant from the Natural Sciences and Engineering Research Council of Canada and by grants from the Canada Foundation for Innovation to FCH.

References

Bartelmehs K.L., Bloss F.D., Downs R.T. and Birch J.B. (1992) Excalibr II. *Zeitschrift für Kristallographie*, **199**, 186–196.

Chaves M.L.S.C. and Scholz R. (2008) Pegmatito Gentil (Mendes Pimentel, MG) e suas paragêneses mineralogical de fosfatos raros. *Revista Escola de Minas*, **61**, 141–149 [in Portuguese].

Chaves M.L.S.C., Scholz R., Atencio D. and Karfunkel J. (2005) Assembleias e paragêneses minerais singulares nos pegmatitos da região de Galiléia (Minas Gerais). *Geociências*, **24**, 143–161 [in Portuguese].

Gagné O.C. and Hawthorne F.C. (2015) Comprehensive derivation of bond-valence parameters for ion pairs involving oxygen. *Acta Crystallographica*, **B71**, 562–578.

Gagné O.C. and Hawthorne F.C. (2016) Bond-length distributions for ions bonded to oxygen: alkali and alkaline-earth metals. *Acta Crystallographica*, **B72**, 602–625.

Gagné O.C. and Hawthorne F.C. (2017*a*) Bond-length distributions for ions bonded to oxygen: Results for the non-metals and discussion of lone-pair stereoactivity and the polymerization of PO_4. Available at: https://chemrxiv.org/articles/Bond-length_distributions_for_ions_bonded_to_oxygen_Results_for_the_non-metals_and_discussion_of_lone-pair_stereoactivity_and_the_polymerization_of_PO4/5410918.

Gagné O.C. and Hawthorne F.C. (2017*b*) Bond-length distributions for ions bonded to oxygen: Metalloids and post-transition metals. Available at: https://chemrxiv.org/articles/Bond-length_distributions_for_ions_bonded_to_oxygen_Metalloids_and_post-transition_metals/5410921.

Gunter M.E. and Twamley B. (2001) A new method to determine the optical orientation of biaxial minerals: a mathematical approach. *The Canadian Mineralogist*, **39**, 1701–1711.

Hawthorne F.C. and Grice J.D. (1990) Crystal structure analysis as a chemical analytical method: application to light elements. *The Canadian Mineralogist*, **28**, 693–702.

Hawthorne F.C. and Huminicki D.M.C. (2002) The crystal chemistry of beryllium. Pp. 333–403 in: *Beryllium: Mineralogy, Petrology and Geochemistry* (E.S. Grew, editor). Reviews in Mineralogy and Geochemistry, **50**. Mineralogical Society of America, Washington DC.

Hawthorne F.C., Ungaretti L. and Oberti R. (1995) Site populations in minerals: terminology and presentation of results of crystal-structure refinement. *The Canadian Mineralogist*, **33**, 907–911.

Huminicki D.M.C. and Hawthorne F.C. (2002) The crystal chemistry of the phosphate minerals. Pp. 123–253 in: *Phosphates: Geochemical, Geobiological, and Materials Importance* (M.J. Kohn, J. Rakovan and J.M. Hughes, editors). Reviews in Mineralogy and Geochemistry, **48**. Mineralogical Society of America, Washington DC.

Mandarino J.A. (1981) The Gladstone – Dale relationship: Part IV. The compatibility concept and its application. *The Canadian Mineralogist*, **19**, 441–450.

Menezes L., Chaves M.L.S.C., Cooper M.A., Ball N., Abdu Y., Sharp R., Hawthorne F.C. and Day M. (2017) Brandãoite, IMA 2016-071a. CNMNC Newsletter No. 39, October 2017, page 1283; *Mineralogical Magazine*, **81**, 1279–1286.

Pedrosa-Soares A.C., Campos C., Noce C.M., Silva L.C., Novo T., Roncato J., Medeiros S., Castañeda C., Queiroga G., Dantas E., Dussin I. and Alkmim F. (2011) Late Neoproterozoic-Cambrian granitic magmatism in the Araçuaí orogen (Brazil), the Eastern Brazilian Pegmatite Province and related deposits. *Geological Society of London Special Publications*, **350**, 25–51.

Scholz R., Chaves M.L.S.C., Belotti F.M., Cândido Filho M. and Menezes Filho L.A.D. (2012) The secondary phosphate minerals from Conselheiro Pena pegmatite district, MG, Brazil: substitutions of tryphylite and montebrasite. Pp. 261–269 in: *Para Conhecer a Terra. Coimbra (Portugal)* (F.C. Lopes, A.I. Andrade, M.H. Henriques, M. Quinta-Ferreira, M.T. Barata and R. Pena dos Reis, editors). Vol. **1**, Imprensa da Universidade de Coimbra, Portugal.

Sheldrick G.M. (2008) A short history of SHELX. *Acta Crystallographica*, **A64**, 112–122.

Yang H., Downs R.T., Evans S.H., Morrison S.M. and Schumer B.N. (2015) Lefontite, IMA 2014-075. CNMNC Newsletter No. 23, February 2015, page 55; *Mineralogical Magazine*, **79**, 51–58.